Autocrine Platelet-Derived Growth Factor–Dependent Gene Expression in Glioblastoma Cells Is Mediated Largely by Activation of the Transcription Factor Sterol Regulatory Element Binding Protein and Is Associated with Altered Genotype and Patient Survival in Human Brain Tumors

Deqin Ma,[1] Catherine L. Nutt,[3] Piam Shanehsaz,[1] Xuejun Peng,[2] David N. Louis,[3] and David M. Kaetzel[1]

[1]Department of Molecular and Biomedical Pharmacology, University of Kentucky College of Medicine and [2]Department of Statistics, University of Kentucky, Lexington, Kentucky and [3]Department of Pathology, Cancer Center and Neurosurgical Service, Massachusetts General Hospital and Harvard Medical School, Boston, Massachusetts

Abstract

A complex profile of gene expression elicited by autocrine platelet-derived growth factor (PDGF) signaling was identified in U87 MG glioblastoma cells by microarray analysis. The most striking pattern observed was a PDGF-dependent activation of at least 25 genes involved with biosynthesis and/or uptake of cholesterol and isoprenoids, including mevalonate pyrophosphate decarboxylase, 3-hydroxy-3-methylglutaryl coenzyme A (HMG-CoA) synthase, HMG-CoA reductase, and low-density lipoprotein receptor. Activity of the HMG-CoA synthase promoter was induced by autocrine PDGF activity as indicated by significant reductions following forced expression of dominant-negative PDGF-A (88%) or treatment with the PDGF receptor antagonist CT52923 (50%). Induction of the HMG-CoA synthase promoter required a binding site for sterol regulatory element binding proteins (SRE-BP), consistent with a key role for these transcription factors in the induction of this gene network. Neither proteolytic activation nor nuclear localization of SRE-BP was affected by disruption of the PDGF autocrine loop, indicating that PDGF signaling is required for other signaling events involved in activation of SRE-BP target genes. Analysis of an expression databank derived from human glial tumors (n = 77) identified a subgroup exhibiting a profile consistent with PDGF dependence, including increased expression of SRE-BP target genes. This subgroup displayed an absence of epidermal growth factor receptor gene amplification, decreased incidence of allelic loss of 10q, increased frequency of TP53 mutations and allelic losses of 1p and 19q, and longer patient survival. This study identifies genes associated with oncogenic activity of PDGF and provides important insights into biomarkers and therapeutic targets in malignant gliomas. (Cancer Res 2005; 65(13): 5523-34)

Introduction

Malignant gliomas are the most common subtype of primary brain tumors, with glioblastoma representing its most malignant form (for a review, see ref. 1). Although glioblastoma is virtually incurable with current treatment modalities, therapeutic prospects have improved with increased understanding of cellular and molecular events underlying its genesis and progression. A frequent hallmark of malignant gliomas is the presence of an autocrine loop involving platelet-derived growth factor (PDGF) ligands and receptors. The PDGF family of ligands consist of four subunits, PDGF-A, PDGF-B, PDGF-C, and PDGF-D, which dimerize via disulfide linkages to form the homodimers PDGF-AA, PDGF-BB, PDGF-CC, and PDGF-DD and the heterodimer PDGF-AB (2–4). Coexpression of PDGF-A and PDGF-B ligands and the α and β isotypes of PDGF receptor (PDGFR) is observed at all stages of glioma progression (5–9). Expression of PDGF-A is increased in glioblastoma (10), suggesting a specific role in tumor progression. More recently, the newly discovered PDGF-C and PDGF-D subunits were also shown to be expressed at high frequency in glioblastoma-derived cell lines and primary human tumor tissues (11). A critical role for PDGF autocrine signaling is indicated by the loss of malignant phenotype in glioblastoma cell lines treated with dominant-negative PDGFs (12–15) and PDGFR antagonists (11, 16).

However, the genes regulated by PDGF autocrine signaling in glial tumors remain unknown. Previous studies of PDGF-induced signaling and gene expression have focused on the acute response to exogenous PDGF, which is unlikely to reflect in all respects the effects of chronic autocrine signaling. Gene expression patterns elicited by the PDGF autocrine loop may also be influenced by interactions with other genes involved in glioma progression. PDGF autocrine signaling becomes more oncogenic with the accumulation of mutations in *TP53* and other genes associated with glioblastoma progression (1). Another factor that must be considered is the well-documented autophosphorylation of immature PDGFRs in v-*sis*-transformed cells, which has been suggested by some as the origin of PDGF-induced signals for mitogenesis and transformation (17, 18). Although signaling from intracellularly activated PDGFRs is dependent on its ultimate arrival at the cell surface (19, 20), intracellular activation could theoretically regulate gene expression quite differently from that via exogenous PDGF ligands.

In the current study, microarray analysis was employed to profile the genes under regulatory control of oncogenic PDGF signaling in

Note: D. Ma and C.L. Nutt contributed equally to this work.

Supplementary data for this article are available at Cancer Research Online (http://cancerres.aacrjournals.org/).

X. Peng is currently at the Department of Biostatistics and Epidemiology, Cleveland Clinic, Cleveland, OH 44195.

Requests for reprints: David Kaetzel, Department of Molecular and Biomedical Pharmacology, University of Kentucky College of Medicine, 800 Rose Street, Lexington, KY 40536-0084. Phone: 859-257-6558; Fax: 859-323-1981; E-mail: dmkaetz@uky.edu.

the glioblastoma-derived cell line, U87 MG (U87; refs. 13, 14). We show that the PDGF autocrine loop is crucial for maintaining a transcriptionally active state for a variety of mitogenesis-related genes (e.g., *FEZ1, TTG-2*, and *CD24* and numerous components of the mevalonate biosynthetic pathway) as well repression of many others, some of which are associated with tumor suppressor functions [e.g., *transforming growth factor-β* (*TGF-β*), *Smad1*, and *thrombospondin-1* (*TSP-1*)]. This pattern of autocrine PDGF-dependent gene expression in cultured cells also has been proven to be a reliable data set for the identification of two subgroups of brain tumor patients, one of which exhibited a PDGF-dependent expression profile that was associated with characteristic genotypic abnormalities and improved patient survival.

Materials and Methods

Cell culture, growth rate, and caspase-8 measurements. The human glioblastoma cell line U87 and stably transfected clonal derivatives were maintained in DMEM (Invitrogen Life Technologies, Carlsbad, CA) supplemented with 10% fetal bovine serum, antibiotics, and nonessential amino acids. For determination of cell growth rates, cells were plated in quadruplicate at a density of 5.0×10^4 cells per 60 mm dish in DMEM containing 10% fetal bovine serum. Eighteen hours later, the medium was replaced with serum-free DMEM and cells were removed by trypsinization at the indicated times of serum deprivation and counted with a hemacytometer. Caspase-8 activity was measured by using a colorimetric assay (BD ApoAlert Caspase-8 Colorimetric Assay kit, BD Biosciences, Mountain View, CA), with all procedures carried out at 4°C. U87 cells were seeded at a density of 1×10^6 cells per 100 mm dish. At indicated time points after serum deprivation, the cells were harvested by centrifugation, lysed in 60 μL cell lysis buffer, and centrifuged at 14,000 × *g* for 10 minutes. The cell lysate (50 μL) was incubated with 2× reaction buffer and caspase-8 substrate at 37°C for 1 hour and the absorbance of the converted substrate was read at 405 nm.

RNA isolation. For analysis of autocrine PDGF loop activity on gene expression, U87 cells and stably transfected clones were initially plated in growth medium at a density of 2.2×10^6 cells in 150 mm dishes. After 48 hours, growth medium was removed and serum-free medium was introduced for 24 hours. For harvesting of total cellular RNA, cells were detached by washing twice with Dulbecco's PBS and incubation in Dulbecco's PBS containing 0.5 mmol/L EDTA at room temperature for 5 minutes. Cells were pelleted by centrifugation at 1,200 × *g* for 5 minutes followed by resuspension in a guanidinium isothiocynate–containing buffer and disruption with QIAshredder homogenizers (Qiagen, Valencia, CA). To examine the effects of exogenous PDGF on gene expression, clone 8.1 cells were plated and depleted of exogenous growth factors by incubation in serum-free medium for 24 hours as described. PDGF-AA and PDGF-BB (Roche, Indianapolis, IN) were then each added to the culture medium at a final concentration of 50 ng/mL. After 24 hours, cells were harvested and total RNA was isolated as described above. RNA was obtained from three replicate dishes for U87 clones 3.1 and 8.1 and from nine dishes for the parent U87 cell line.

Oligonucleotide microarray analysis. Gene chip analyses were done by the University of Kentucky Microarray Core Facility following the protocols described in the Affymetrix manual (Affymetrix, Inc., Santa Clara, CA). Briefly, double-stranded cDNA was synthesized from 5 μg total RNA using T7-(dT)24 as primer (Invitrogen, Carlsbad, CA). cRNA was then produced in an *in vitro* transcription reaction (Affymetrix, P/N900182) and biotinylated by the Bioarray High-Yield RNA Transcript Labeling kit (Affymetrix). Labeled targets (20 μg/sample) were fragmented and hybridized to human U95 probe arrays (one chip per RNA sample) in a rotating oven at 45°C. Chips were washed and stained with streptavidin phycoerythrin on a fluidics station and scanned twice at 570 nm in a confocal scanner (Agilent Affymetrix GeneArray Scanner) at a resolution of 3 μm.

Data analysis. The preliminary data normalization and standardization and data analyses were done using Affymetrix Microarray Suite version 5.0 (http://www.affymetrix.com). Briefly, for each probe set, Microarray Suite version 5.0 computes the signal based on the Tukey's biweight average of the differences between each of perfect match/mismatch probe pairs, which is approximately proportional to the gene expression level. Absent and present calls for each probe set were based on the Wilcoxon signed rank test of 11 perfect match/mismatch probe pairs, employing the default detection *P* threshold of absent or present calls as 0.05. To control for false-positive rates, we used the "absent/present" calls as the first filtering criteria. Among the 12,625 probe sets used in the analysis of expression profiles for serum-deprived U87 cells, genes with less than three "present" calls among either group were excluded from the overall statistical analysis. For the remaining 7,128 probe sets, two-sample *t* tests were done between the two treatments with $n = 3$ for clones 3.1 and 8.1 and $n = 9$ for the parent cells. To obtain a practical balance of false-positive rate and false-negative rate control (21), only genes with $P \leq 0.01$ and fold change ≥ 2.0 were included in Table 1 and Supplementary Table S1. Preliminary data analyses were done with Affymetrix Microarray Suite version 5.0 and Data Mining Tools. Data analyses of glial tumor samples (22) used GeneCluster (http://www-genome.wi.mit.edu/cancer/software/software.html). Statistical analyses were done using SAS version 8.2 and S-Plus version 6.0. Genes were assigned to functional categories using the database provided by Affymetrix (see http://www.netaffx.com).

Transient transfection and reporter gene assays. U87 cells and stably transfected clones were seeded into 24-well plates and cotransfected using LipofectAMINE reagent (Invitrogen) with the SRE-containing luciferase reporter plasmid, pSynSRELuc (generously provided by T. Osborne, University of Texas-Southwestern). Interwell variation in transfection efficiency was quantified by cotransfection with the *Renilla* luciferase plasmid, pRL-TK (Promega, Madison, WI). Firefly and *Renilla* luciferase activities were measured in a 96-well plate reader (TR-717, Applied Biosystems, Foster City, CA), with reporter gene activity presented as the ratio of firefly to *Renilla* activities (relative luciferase activity).

Immunofluorescence and confocal microscopy. U87 cells were plated at a density of 1.5×10^5 on 35 mm polylysine-treated dishes and exposed to the indicated duration of serum deprivation. For fixation, cells were washed with PBS, treated with 4% formaldehyde for 10 minutes, and permeabilized with 0.3% Triton X-100 for 10 minutes. After blocking in 10% goat serum and 1% bovine serum albumin for 1 hour, the cells were incubated with 1 μg/μL anti–sterol regulatory element (SRE) binding protein (SRE-BP)-1a (Santa Cruz, Santa Cruz, CA) for 1 hour. After washing thrice with PBS, cells were incubated with FITC-conjugated goat anti-rabbit antibody (Santa Cruz) for 1 hour in the dark. Cells were then washed with PBS and the nuclear staining dye H-33342 (0.1 μg/mL in PBS/0.05% bovine serum albumin) was added to the cells. Fixation, antibody incubations and washing steps were done at room temperature. Images were acquired using a confocal microscope (RCM 8000, Nikon, Melville, NY) with a CF Fluor ×40 water immersion objective and analyzed with the program MetaMorph (Universal Imaging, West Chester, CA). Red pseudocolor was used for the nuclear staining and green was used for fluorescent stain.

Supplementary data. Additional results, including comprehensive spreadsheets displaying all genes altered significantly by PDGF (autocrine and exogenous), statistical flow charts, volcano plots of differential gene expression, validation of microarray assessments of mRNA levels by reverse transcription-PCR (RT-PCR), and immunoblot analysis of selected gene products are available in Supplementary Data.

Results

Genes regulated by autocrine platelet-derived growth factor signaling in the human glioblastoma cell line, U87 MG. To identify genes regulated by autocrine PDGF signaling, we employed microarray analysis to compare gene expression profiles in the presence and absence of an active PDGF loop in the human glioblastoma cell line, U87. For this purpose, we employed a stably transfected U87 clone (8.1) that overexpresses a dominant-negative form of the PDGF-A subunit (A^{dn}; ref. 14). The mutation employed

Table 1. Summary of genes differentially expressed between U87 and clone 8.1 cells

	Induced by autocrine PDGF				Repressed by autocrine PDGF (increased in 8.1)			
	Genbank accession no.	Gene*	Fold change†	Regulation in glioma cluster 1‡	Genbank accession no.	Gene	Fold change	Regulation in glioma cluster 1
Growth/cytokines/ apoptosis	U60060	*FEZ1*	41.8	Up	X14787	*TSP-1* ($P = 0.028$)§	9.2	—
	X61118	*TTG-2*	15.1	Down	Z24680	*Garp* ($P = 0.04$)	3.8	—
	D80010	*Lipin 1*	4.6	Up	AF100779	*WISP1*	3.0	Down
	AB017563	*IGSF4*	4.2	Down	M69199	*G0S2*	2.9	Down
	AF001294	*TSSC3*	4.1	Down	AI701049	*Guanine exchange factor (cdc24)*	2.8	—
	D38503	*PMS8*	3.3	—	L13720	*GAS6*	2.5	—
	AI632589	*LOH11CR2A*	2.7	Up	U09278	*Fibroblast activator protein*	2.5	Down
	L19183	*Mac30* ($P = 0.038$)	2.2	—	AL080177	*Ubiquitin-like 3 (UBL3)*	2.1	Up
	AB008822	*Osteoclastogenesis inhibitory factor*	2.2	—	U83508	*Angiopoietin-1*	2.1	Down
	M74297	*Homeobox 1.4 protein*	2.1	—	S69790	*Brush-1*	2.1	Up
					AF059611	*Nuclear matrix protein NRP/B*	2.0	—
Adhesion/ECM	X71345	*Trypsinogen IV b-form*	5.0	—	L35594	*Autotaxin*	2.9	—
	U66061	*Trypsinogen C*	3.9	—	X05610	*Type IV collagen α(2)*	2.5	Down
	M77016	*Tropomodulin*	3.8	—	X83535	*MT-MMP*	2.5	—
	U03272	*Fibrillin-2*	3.2	Down	X13839	*Vascular smooth muscle α-actin*	2.4	Down
	D82345	*Neuroblastoma thymosin β*	3.1	—	M31165	*Tumor necrosis factor–inducible 6*	2.4	—
	AI445461	*TM4SF1*	2.8	Down	AI140857	*Laminin NH_2-terminal (domain VI)*	2.1	Down
	D32039	*Proteoglycan M (versican 3)* ($P = 0.016$)	2.5	—	M24283	*ICAM, major rhinovirus receptor* ($P = 0.041$)	2.1	—
	L13616	*FAK*	2.5	—	U17760	*LAMB3*	2.1	—
	X15998	*Proteoglycan PG-M (versican 1)*	2.3	—		*Fibronectin*	2.0	—
	AF063002	*SLIMMER*	2.2	—	U68186	*ECM protein 1*	2.0	—
Metabolism‖	U49260	*MPD*	37.0	—	AF05921	*Cholesterol 25-hydroxylase*	7.4	Down
	X66435	*HMG-CoA synthase*	23.1	Up	D86181	*Galactocerebrosidase*	3.1	—
	AL050118	*FADS2*	10.3	Up	X60708	*Liver dipeptidyl peptidase IV*	2.5	Down
	U60205	*Methyl sterol oxidase (ERG25)*	7.8	Up	U77604	*MGST2*	2.4	Down
	Y13647	*Stearoyl-CoA desaturase*	6.7	—	U32989	*Tryptophan oxygenase (TDO)*	2.4	—
	X69141	*Squalene synthase*	6.4	Up	L25879	*Epioxide hydrolase (EPHX1)*	2.1	Up
	D13643	*24-Dehydrocholesterol reductase*	5.8	—				
	L00352	*LDL receptor*	5.3	—				
	U29344	*Breast carcinoma fatty acid synthase*	5.1	Up				
	U96876	*INSIG-1*	5.0	Up				
	M11058	*HMG-CoA reductase*	4.8	Up				
	AJ002962	*HB-FABP*	4.8	Down				
	U13697	*IL1BCE*	4.6	—				

(Continued on the following page)

Table 1. Summary of genes differentially expressed between U87 and clone 8.1 cells (Cont'd)

	Induced by autocrine PDGF				Repressed by autocrine PDGF (increased in 8.1)			
	Genbank accession no.	Gene*	Fold change†	Regulation in glioma cluster 1‡	Genbank accession no.	Gene	Fold change	Regulation in glioma cluster 1
	X17025	*IPP isomerase*	4.6	Up				
	D84307	*Phosphoethanolamine cytidylyl transferase*	4.4	—				
	S70154	*Acetoacetyl-CoA thiolase*	4.0	—				
	D78130	*Squalene epoxidase*	3.9	Up				
	D14697	*Farnesyl diphosphate synthase FDPS*	3.7	—				
	W26480	*C-5 sterol desaturase*	3.7	Up				
	U06715	*Cytochrome B561*	3.7	—				
	AF034544	*Δ7-Sterol reductase*	3.6	—				
	D89053	*Acyl-CoA synthetase 3*	3.4	—				
	AF038664	*β-1,4-galactosyltransferase*	3.3	—				
	AC004770	*FADS1*	3.2	Up				
	U23942	*CYP51 (lanosterol 14α-demethylase)*	3.1	—				
Transcription/ DNA repair/ replication					D50370	*Nucleosome assembly protein 1–like 3*	3.8	Up
					X98834	*Hsal2*	2.1	Up
					U66619	*SWI/SNF complex 60-kDa subunit*	2.0	
					X59373	*HOX4D*	2.0	
Oncogenes	U03735	*MAGE-3 antigen*	5.8		J04152	*GA733-1*	3.2	Down
	U18914	*TPD52*	4.6	Up				
	M90657	*Tumor antigen L6*	2.7					
Receptors/signal transduction	L33930	*CD24*	28.3		X14885	*TGF-β3*	5.2	Down
	U87460	*G protein-coupled receptor 37*	22.8	Down	Z24680	*RAR-β* (π = 0.044)	3.8	Down
	Y07593	*CAR protein*	22.2		AL008583	*Neuronal pentraxin receptor*	3.2	Up
	S62907	*GABA receptor α2*	9.6		U59423	*Smad1*	3.1	Down
	M38690	*CD9 antigen*	6.8		AB017363	*Frizzled-1*	2.7	
	D25538	*Adenylate cyclase 7 (ADCY7)*	3.1		AB002367	*MAPK ERK2 ARK2*	2.6	
	L13616	*Protein tyrosine kinase 2 (PTK2)*	2.5	Up	X89399	*Ins(1,3,4,5)P4 binding protein*	2.4	
					Z24680	*RAR responder 3*	2.4	
					U97669	*Notch 3*	2.3	Down
					U31382	*G protein γ4 subunit*	2.3	Up
					M69043	*Mad 3*	2.2	
					J03258	*Vitamin D receptor*	2.2	
					X54134	*Tyrosine phosphatase, ϵ*	2.1	
					AL049801	*Novel gene, similar to rat RhoGAP*	2.1	Down
					AF060219	*Guanine exchange factor (RLG)*	2.1	Up
					D45248	*HUMPHPA28A*	2.1	Down
Miscellaneous	U16954	*AF1q*	3.1	Up	AJ224979	*MTMR1*	3.1	Up
	X92841	*MICA*	2.6		U83659	*MDR protein 3 (MRP3)*	2.2	Down
	M59830	*HSP70-2*	2.5		AJ010071	*TOM1-like protein*	2.3	
	AB026118	*MALT1*	2.2	Down	X71661	*ERGIC-53*	2.3	

(Continued on the following page)

Table 1. Summary of genes differentially expressed between U87 and clone 8.1 cells (Cont'd)

Induced by autocrine PDGF				Repressed by autocrine PDGF (increased in 8.1)			
Genbank accession no.	Gene*	Fold change†	Regulation in glioma cluster 1‡	Genbank accession no.	Gene	Fold change	Regulation in glioma cluster 1
U04735	*Stch*	2.1		AF039555	*Visinun-like protein 1 (VSNL1)*	2.1	
U70671	*Ataxin-2-related protein*	2.0	Up				
AJ011712	*TNNT1*	2.0					

*Annotation from NetAffx (http://www.affymetrix.com).
† Average ratio calculated as described in Materials and Methods.
‡ Direction of regulation for genes in glioma cluster 1 that exhibited significant alterations in expression relative to cluster 2.
§Genes with $0.01 < P < 0.05$ were retained in Table 1 and their corresponding *P*s shown in parentheses if they were also shown to be regulated by exogenous PDGF in Supplementary Table S2. Other exceptions to the filtration criteria of $P < 0.01$ and >2-fold response were those genes for which differences in mRNA expression were validated by RT-PCR (Supplementary Fig. S2A).
‖Only genes with >3.0-fold induction in the category of "Metabolism" are displayed.

does not interfere with dimerization but renders the molecule unable to bind PDGFRα and PDGFRβ and unable to bind heparin or induce mitogenesis (14, 23). Clone 8.1 cells grow normally in serum-supplemented medium but, unlike parent U87 cells, are dependent on exogenous growth factors and grow poorly when explanted into athymic nude mice. In addition to the parent U87 cells and clone 8.1, another U87 clone (3.1) that expresses a G418 resistance marker but no other heterologous gene product was also subjected to microarray analysis. To specifically examine the effects of autocrine PDGF loop activity, wild-type U87 and clone 3.1 and 8.1 cells were depleted of exogenous growth factors by 24 hours of serum withdrawal. By interfering with formation of biologically active PDGF, the A^{dn} polypeptide blocks both the classic autocrine PDGF loop and the putative internal ("intacrine") activation of PDGFRs (Fig. 1).

As seen previously, serum deprivation inhibited proliferation of clone 8.1 cells, whereas parent U87 cells and a neo^r-stable transfectant (clone 3.1) continued to divide robustly (Fig. 2*A* and *B*). Morphologic examination of the serum-deprived clone 8.1 cells revealed no overt signs of apoptotic or necrotic cell death, such as membrane ruffling, for up to 7 days in culture. Caspase-8 activity, an early marker of apoptosis, was not significantly different between the three cell lines for up to 72 hours of serum deprivation (Fig. 2*C*). Taken together, these findings strongly suggest that the expression patterns identified in serum-deprived clone 8.1 cells are indeed the result of disrupted PDGF autocrine activity and not secondary to a generalized apoptotic response.

Gene expression patterns in parent U87 and clone 3.1 cells were not different statistically ($P \leq 0.01$) and were thus pooled into one control group for comparison with that obtained in clone 8.1 cells (see Materials and Methods). Statistical analysis revealed a total of 594 genes that were differentially expressed ($P < 0.01$) between clone 8.1 cells and the pooled control group (parent plus clone 3.1; Supplementary Table S1A). At this level of stringency, only 72 false-positive genes would have been expected, strongly suggesting that the majority of the identified genes were indeed regulated by disruption of the PDGF autocrine loop. As a further protection against false positives, the additional criterion of >2-fold change was applied. This filtering yielded a total of 129 genes that were differentially expressed; 78 were up-regulated in clone 8.1, whereas 51 were down-regulated. Table 1 displays a list of these genes, subdivided into seven functional groups using the NetAffx version of the Gene Ontology database. For clarity, mRNAs that were down-regulated in clone 8.1 cells will heretofore be designated as "induced by autocrine PDGF" (i.e., repressed by A^{dn} expression) and mRNAs up-regulated in clone 8.1 cells as "repressed by autocrine PDGF". mRNAs encoding proteins with metabolic functions constituted the largest group ($n = 42$) followed by receptors and signal transduction ($n = 29$), growth ($n = 21$), adhesion and extracellular matrix (ECM; $n = 19$), oncogenes ($n = 5$), transcription ($n = 4$), and miscellaneous ($n = 14$). Whereas a few of these differentially regulated mRNAs have been shown previously to be regulated in fibroblasts by exogenous PDGF treatment (24), a large majority is unique. The latter is thus likely to represent a broad spectrum of genes uniquely regulated in the U87 cell line by chronic PDGF autocrine activity. Representative differentially

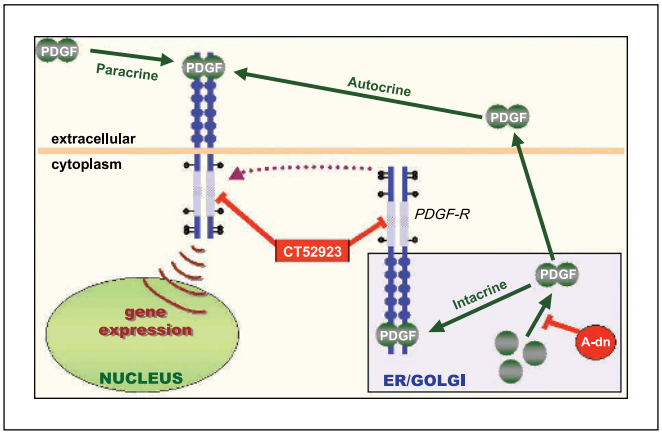

Figure 1. Targeting of PDGF growth loops in U87 cells with dominant-negative PDGF-A and the PDGFR inhibitor, CT52923. Dominant-negative PDGF-A (A^{dn}) blocks formation of active PDGF dimers within the ER, which in turn prevents both the internal activation ("intacrine") of PDGFRs and the secretion of PDGF into the extracellular space ("autocrine" and "paracrine"). CT52923 also blocks intacrine and extracellular routes of the ligand-activated autotyrosine kinase activity of PDGF-R.

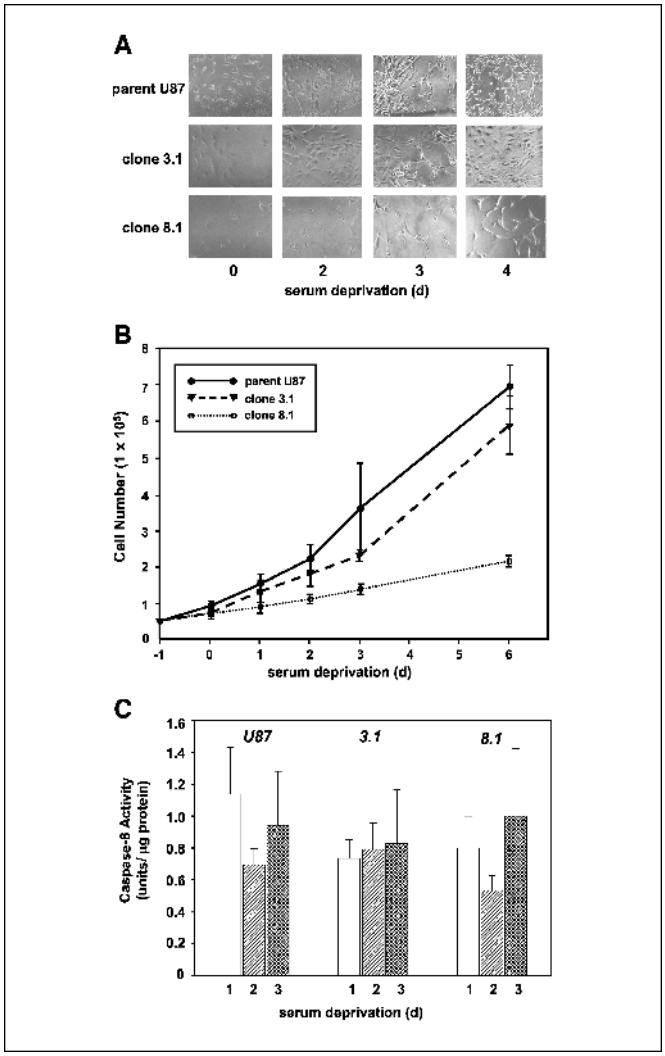

Figure 2. Effects of serum deprivation on cell growth, morphology, and apoptosis. *A,* U87 cells (parent, clone 3.1, and clone 8.1) were plated, subjected to the indicated lengths of serum deprivation, and analyzed by Nomarski interference microscopy as described in Materials and Methods. *B,* cells were subjected to serum deprivation as in (*A*) and counted directly with a hemacytometer. *C,* caspase-8 activity was determined in the U87 cell lines as a measure of apoptotic activity over a 3-day time course of serum deprivation.

expressed mRNAs (eight repressed and eight induced) were further examined by RT-PCR, and in each case, the results confirmed the microarray analysis (Supplementary Fig. S1A). Immunoblot analysis (Supplementary Fig. S1B) showed the expected patterns of protein expression for each of three up-regulated genes [*GAS6, retinoic acid receptor-β* (*RAR-β*), and *Smad1*] and three down-regulated genes [*CD9, low-density lipoprotein receptor* (*LDL receptor*), and *steroyl CoA reductase*].

Disruption of the PDGF autocrine loop in clone 8.1 resulted in nearly equal numbers of up-regulated and down-regulated mRNAs in the functional group of growth factors, cytokines, and apoptosis-related proteins (Table 1). Consistent with the growth-promoting activity of PDGF, two growth-stimulatory mRNAs (*TTG-2* and *lipin 1*) were induced by PDGF autocrine activity. The most prominent induction was that of *TTG-2* (15-fold), a development-relevant molecule frequently overexpressed in T-cell leukemia as a consequence of chromosomal translocation (25). The majority of the PDGF-induced mRNAs (*FEZ1, IGSF4, TSSC3, PMS8, LOH11-CR2A*, and *Mac30*) were actually associated with tumor suppressor functions. *FEZ1*, a leucine zipper protein associated with tumor suppressor activity in multiple cancers (26), was the most highly induced mRNA in the overall analysis (42-fold). Also counter to expectations, the majority of PDGF-repressed mRNAs (*Garp, WISP1, G0S2, GAS6, fibroblast activator protein*, and *angiopoietin-1*) were associated previously with growth stimulation. *TSP-1* and *brush-1* were growth/tumor suppressor molecules that were identified to be under repressive control of PDGF activity. *TSP-1* is an ECM glycoprotein involved in tissue remodeling and a well-characterized angiogenesis inhibitor and tumor suppressor in glioblastoma (27–29).

Two mRNAs encoding ECM proteins associated with antiangiogenic and antimetastatic activities (30, 31), *type IV collagen* and *LAMB3*, were shown to be under PDGF-mediated repression. The majority of PDGF-repressed mRNAs in this class [*autotaxin, membrane-type matrix metalloproteinase* (*MT-MMP*), *vascular smooth muscle α-actin, laminin, fibronectin*, and *ECM protein 1*], however, are associated primarily with stimulation of growth. As expected, most mRNAs within this class that were induced by PDGF autocrine activity are associated with growth, oncogenesis, and/or malignant progression. These included the *trypsinogen IV, trypsinogen C, neuroblastoma thymosin β, TM4SF5*, and three molecules associated with focal adhesion, *FAK*, two isotypes of *proteoglycan M* (*versican V1* and *versican V3*), and *SLIMMER*. One PDGF-induced mRNA, cytoplasmic antiproteinase 2, is a serine protease inhibitor implicated as angiogenesis inhibitor (32).

The most profound effect resulting from disruption of PDGF autocrine activity was an induction of mRNAs encoding enzymes required for cholesterol and isoprenoid synthesis. Many of these represented known regulatory targets of SRE-BPs (for review, see ref. 33). Of particular note in this group was *IL1BCE*, an enzyme implicated in SRE-BP activation (34). *Cholesterol 25-hydroxylase* mRNA was repressed by PDGF, consistent with its proposed role in suppression of SRE-BP activation (35).

Expression of four transcription-related factors, nucleosome assembly protein 1–like 3, the homeotic factors *HOX4D* and *Hsal2*, and the 60-kDa subunit of *SWI/SNF complex*, was repressed modestly by PDGF autocrine activity. An interesting pattern of coordinate up-regulation (~5- to 6-fold) was observed with the melanoma surface antigens *MAGE-3* and *MAGE-12* (36) and *TPD52*, a pattern of coexpression noted previously in breast carcinoma (37). Also up-regulated were two other oncogenic proteins, *Tls/CHOP* and *tumor antigen L6*. *GA733-1* (or *Trop-2*), a putative cell surface receptor involved in cell adhesion and shown to be overexpressed in many carcinomas (38), was down-regulated.

Expression of mRNAs encoding numerous receptors and signal transduction molecules were regulated by PDGF autocrine activity, with most being repressed. Down-regulated target genes included *TGF-β3* and its cognate second messenger *Smad1, RAR-β*, several G proteins and related molecules [*G protein γ4 subunit, RhoGAP-like gene*, and *guanine exchange factor* (*RLG*)], *extracellular signal-regulated kinase 2* (*ERK2*), *IP4 binding protein, frizzled-1*, and *Notch 3*. Up-regulated genes were fewer, but the magnitude of up-regulation was quite high for many, especially for *CD24* (28-fold), the endothelin receptor–like molecule *G protein-coupled receptor 37* (23-fold), and the adenoviral receptor *CAR protein* (22-fold). The marked PDGF-mediated up-regulation of *CD24* was of particular interest, as this molecule has been specifically implicated as a promoter of malignant growth in glioblastomas (39). Also of interest were strong inductions of mRNAs encoding *GABA receptor*

α2 (10-fold) and *CD9* (7-fold), the former noted previously as being frequently overexpressed in gliomas (40).

Reactivation of platelet-derived growth factor signaling in clone 8.1 cells with exogenous platelet-derived growth factor results in a gene expression profile similar to but distinct from that elicited by autocrine platelet-derived growth factor activity. The initial microarray study represented an analysis of gene expression mediated by the sum of external and intacrine modes of PDGFR activation because overexpression of the A^{dn} polypeptide interrupts both (Fig. 1). To assess gene expression patterns elicited selectively by the external PDGF loop alone, we next examined the effects of exogenous PDGF treatment in serum-depleted clone 8.1 cells. Cells were treated with both PDGF-AA and PDGF-BB to stimulate both PDGFRα and PDGFRβ isotypes, as both seem to be activated in U87 and many other glioblastoma cell lines (11). The two experimental groups (± PDGF) were subjected to the same filtering paradigm used in the comparison of control U87 and clone 8.1 cells.

A marked preponderance of genes were up-regulated by PDGF treatment in five of the six functional categories (for summary, see Supplementary Table S1B), a trend not seen in the initial study (Table 1). Also notable was the relatively small overlap in these genes with those regulated by autocrine PDGF activity (21 of 129); these genes and the directions and extent of their regulation are identified in Table 1. Interestingly, the direction of regulation was retained for each. Most of the overlap occurred in genes associated with cholesterol/isoprenoid biosynthesis and transport (11 of the 25 genes under autocrine control). This overlap and the recapitulation of positive or negative regulation in each of those genes provided considerable validation to the dominant-negative approach used to disrupt PDGF autocrine activity. Nevertheless, in functional categories other than metabolism, most of the genes regulated by exogenous PDGF were distinct from those regulated by autocrine PDGF. This strongly suggests that autocrine stimulation elicits unique patterns of PDGF signaling, probably secondary to the chronic nature of the stimulus and/or the added component of intacrine receptor activation.

One of the most notable outcomes of the analysis was the induction in numerous proteins involved in cell cycle control, such as cyclins (A, B1 and B2, and D2), cyclin-dependent kinase 1, multiple CDCs (2, 5, 6 and 25), ASK (activator of CDC7 kinase), p19INK4d, and the cyclin-selective ubiquitin-conjugating enzyme UbcH10. Interestingly, none of these had been identified as up-regulated by PDGF autocrine activity in the earlier analysis. However, *TSSC3* and *Mac30* were two up-regulated mRNAs that were identified previously as induced by PDGF autocrine stimulation. Similarly, *Garp* was repressed by exogenous PDGF, as it was by PDGF autocrine activity. Expression of *proteoglycan M* and two integrins (α_2 and α_{6B}) was induced by exogenous PDGF, whereas *intercellular adhesion molecule* (*ICAM*) was repressed, as seen earlier with these autocrine PDGF-regulated ECM proteins. Ten of the 13 most highly induced metabolism-related mRNAs were involved with synthesis and/or uptake of cholesterol and isoprenoids. Moreover, each had been identified in the previous analysis as induced by autocrine PDGF activity as well. The fold induction for most of these mRNAs was remarkably similar to that elicited by the PDGF autocrine loop (e.g., *MPD*: autocrine PDGF, 37-fold; exogenous PDGF, 33-fold). Several factors involved with DNA repair and replication, such as DNA topoisomerase II, TCF8, DNA polymerase α, replication factor C, DNA-dependent protein kinase, and chromatin assembly factor-1, were induced by PDGF treatment. Liver X-activated receptor α expression was repressed, noteworthy in light of the key role played by liver X-activated receptors in the stimulation of SRE-BP-1c gene transcription (41) and possible activation of a negative feedback loop. The tumor suppressor BRCA1 was also induced, as was BARD1, a so-called RING protein that interacts with the NH_2 terminus of BRCA1 and has been implicated in the tumor suppression mechanism (42). *GA733-1* represented an oncogenic factor that was identified in both analyses to be under the repressive influence of PDGF. A wide range of different receptors and signaling molecules were regulated by exogenous PDGF, with nearly equal numbers of them being induced or repressed. All of the mRNAs induced by the PDGF treatment were distinct from those identified as under autocrine control in the previous analysis. Several these would be considered to play important roles in mitogenic signaling, such as the tumor-amplified kinase BTAK (43), MAPKKK5 (ASK1), IP3 kinase, Pak1, Sprouty 2, and SAK. The latter was noteworthy, in light of its identity as an effector of the intracellular tyrosine kinase EMT (44), which was also up-regulated by PDGF. Interestingly, expression of PDGFRα was significantly up-regulated by exogenous PDGF. In contrast with the induced mRNAs, many of those repressed by PDGF were indeed identified as such in the previous analysis. These included *angiopoietin-1, RAR-β, TGF-β3*, and a RhoGAP-like protein. TGF-β2 was also repressed, in keeping with the overall trend toward an important action of PDGF in down-regulating this growth-suppressing signal pathway.

Platelet-derived growth factor autocrine activity induces sterol regulatory element binding protein–mediated transcription in U87 glioblastoma cells. The coordinate induction of numerous mRNAs encoding enzymes involved in synthesis or transport of cholesterol and isoprenoids by PDGF autocrine activity suggested activation of the SRE-BPs. SRE-BPs are basic helix-loop-helix leucine zipper proteins that regulate lipid homeostasis by directly stimulating transcription of at least 30 different genes (34). On proteolytic activation in the endoplasmic reticulum (ER) membrane, SRE-BPs translocate to the nucleus and stimulate transcription of target genes via binding to specific DNA sequence motifs (SRE). To determine whether SRE activity was stimulated by the PDGF autocrine loop in U87 cells, activity of a prototype SRE from the 3-hydroxy-3-methylglutaryl coenzyme A (HMG-CoA) synthase gene (−324 to −225) was compared in clone 3.1 and 8.1 cells. SRE activity was measured by transient transfection with the luciferase reporter plasmid, pSynSRELuc (45), which consists of the HMG-CoA synthase SRE fused to a minimal HMG-CoA synthase promoter fragment. U87 clones 3.1 and 8.1 were transiently transfected with pSynSRELuc for 24 hours in serum-containing medium followed by transfer into serum-free medium and measurement of luciferase accumulation (Fig. 3*A*). Luciferase activity accumulated to higher levels in clone 3.1 over a 48-hour time course, consistent with induction by the intact autocrine PDGF loop in clone 3.1 (and, conversely, loss of stimulation when the loop was disrupted in clone 8.1). Most of the activity in clone 8.1 cells was attributable to the basal promoter and not the SRE enhancer (data not shown). We also examined the effect of the tyrosine kinase inhibitor CT52923 (kindly provided by N. Lokker, Millenium Pharmaceuticals, South San Francisco, CA), which possesses a high degree of selectivity for the PDGFRα and PDGFRβ isotypes (and to a lesser extent the closely related c-*kit*; ref. 46) and should block both external and internal pathways of PDGFR signaling. A dose-dependent inhibition of SRE activity was

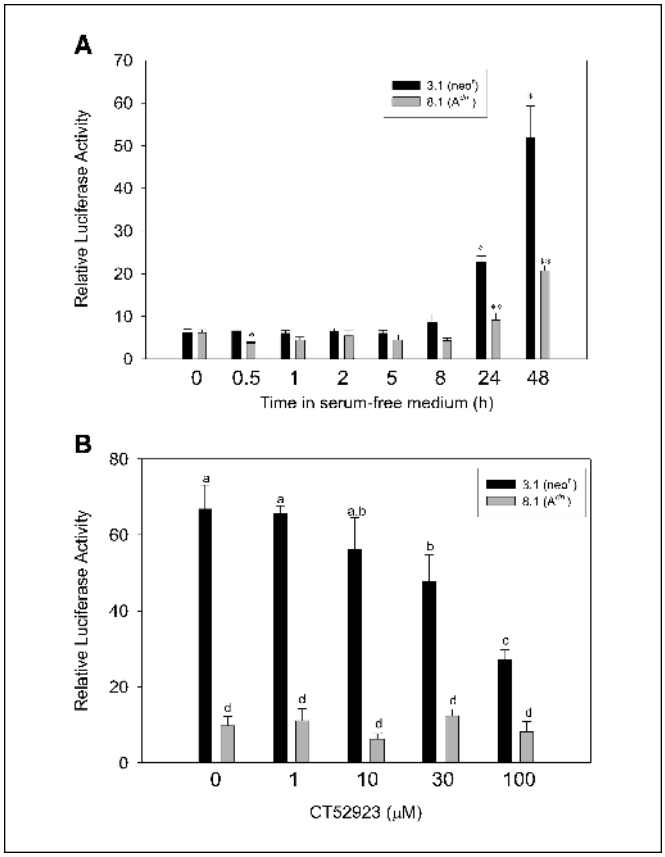

Figure 3. PDGF autocrine signaling stimulates transcription via the SRE of the HMG CoA synthase promoter. *A,* clone 3.1 and 8.1 cells were transfected in duplicate with the SRE-containing reporter plasmid, pSynSRELuc, and then exposed to the indicated times of serum deprivation and harvested for measurement of luciferase activity. Results are expressed in terms of relative luciferase activity, which has been corrected for variation in transfection efficiency. *Columns,* mean from three replicate experiments; *bars,* SE. *, $P < 0.05$, significant increase in luciferase activity for 3.1 cells relative to values obtained at the start of the experiment (time 0). **, $P < 0.05$, significant increase in 8.1 cells relative to time 0 as well as a significant decrease relative to the corresponding treatment time for 3.1 cells. *B*, cells were transfected with pSynSRELuc for 24 hours and then serum starved for 24 hours with the indicated concentrations of the PDGFR inhibitor, CT52923. Values not sharing a common superscript (a-d) are significantly different from one another.

observed in serum-depleted clone 3.1 cells treated with CT52923, detectable at drug concentrations of 30 and 100 μmol/L (Fig. 3*B*). This inhibition was not observed in clone 8.1 cells, demonstrating the selectivity of the drug for PDGF-mediated signaling. Taken together, these observations indicate that autocrine PDGF activity induces a program of cholesterol/lipid homeostatic genes via activation and binding of SRE-BP to SREs within the regulatory regions of those genes.

Immunocytochemical analysis of SRE-BP-1a revealed no obvious difference in nuclear localization of the transcription factor between clone 3.1 and 8.1 cells over a 48-hour time course of serum deprivation (Fig. 4*A*). Additional immunoblot analysis of both clone 3.1 and 8.1 cells after 4 hours of serum deprivation revealed that most of the SRE-BP-1a was present in the nuclear debris fraction as the mature, fully processed form of the protein (~72 kDa; mSRE-BP-1a). Smaller amounts of the unprocessed precursor (pSRE-BP-1a) also appeared in the nuclear debris fraction of both cell lines, probably reflecting the presence of significant amounts of ER (Fig. 4*B*). Small amounts of pSRE-BP-1a were also found in the cytosol, membrane, and nuclear extract fractions of both clones. Similar trends were observed after 24 hours of serum deprivation, with perhaps subtly higher amounts of pSRE-BP-1a present in the nuclear debris fraction of clone 8.1 cells. Overall, the ratio of membrane-associated to nuclear mSRE-BP-1a was not significantly different between clone 3.1 and 8.1 cells, indicating that proteolytic cleavage and nuclear translocation of SRE-BP-1a proceeds unimpaired in the absence of PDGF autocrine signaling. No evidence of alternate molecular weight forms consistent with PDGF-evoked phosphorylation of SRE-BP-1a was evident. Taken together, these observations strongly suggest that PDGF autocrine signaling does not activate SRE-BP per se. Instead, such signaling may activate cooperatively acting PDGF response elements in the promoters of SRE-containing target genes or perhaps cofactors functioning in concert with SRE-BP.

Autocrine platelet-derived growth factor–dependent gene expression patterns in U87 cells identify two distinct classes of brain tumors. Having identified a profile of gene expression regulated by autocrine PDGF loop activity in cultured U87 cells, we next assessed its relevance to expression patterns in human brain tumor tissues. To this end, the collection of autocrine PDGF-regulated genes (total of 127: 75 up-regulated and 52 down-regulated) was used to screen an expression profile databank derived from 77 high-grade gliomas (Supplementary Table S1A) for the presence of tumor subgroups exhibiting expression patterns consistent with PDGF-dependent control. Unsupervised SOM clustering analysis identified two highly stable tumor subclasses, with 65% (83 of 127) of the autocrine PDGF-regulated genes expressed at different levels between them ($P \leq 0.05$). The larger of these clusters (cluster 1) contained 50 gliomas and was composed of 14 glioblastomas, 31 anaplastic oligodendrogliomas, and 5 anaplastic oligoastrocytomas, whereas cluster 2 contained 20 glioblastomas and 7 anaplastic oligodendrogliomas. Strength of the clustering was high, with leave-one-out cross-validation demonstrating an accuracy of 97.4% (75 of 77 correct calls). Most genes induced by autocrine PDGF activity in U87 cells were similarly up-regulated in cluster 1 tumors [18 of 26 (69%); Table 1]. This correlation was attributable in large part to metabolism-related genes (11 up-regulated genes of 12), particularly those involved in cholesterol and lipid homeostasis. Conversely, most of the genes classified as down-regulated by autocrine PDGF activity were also expressed at lower levels in cluster 1 [16 of 25 (64%); Table 1]. Interestingly, both PDGF-A and PDGFRα were down-regulated significantly in cluster 1 relative to cluster 2, suggesting perhaps a compensatory response to chronic activation of the PDGF autocrine loop in these tumors. When clusters 1 and 2 were analyzed for their overall gene expression patterns against the entire U95A probe list, more striking changes were apparent (data not shown). Taken together, this analysis identified a major subgroup of patients (cluster 1) whose tumors exhibited a gene expression profile highly consistent with PDGF-dependent transcriptional control. It was noteworthy that most of these PDGF-dependent tumors were anaplastic oligodendrogliomas and anaplastic oligoastrocytomas, because the U87 cell line was originally derived from a glioblastoma tumor. On the other hand, the distinction between these clusters was not absolute, with glioblastomas still constituting a significant proportion of cluster 1 tumors (28%). Screening of the same glioma expression databank with the gene expression profile derived from treatment of U87 cells with exogenous PDGF also yielded two highly accurate and stable clusters of gliomas. However, neither of these clusters

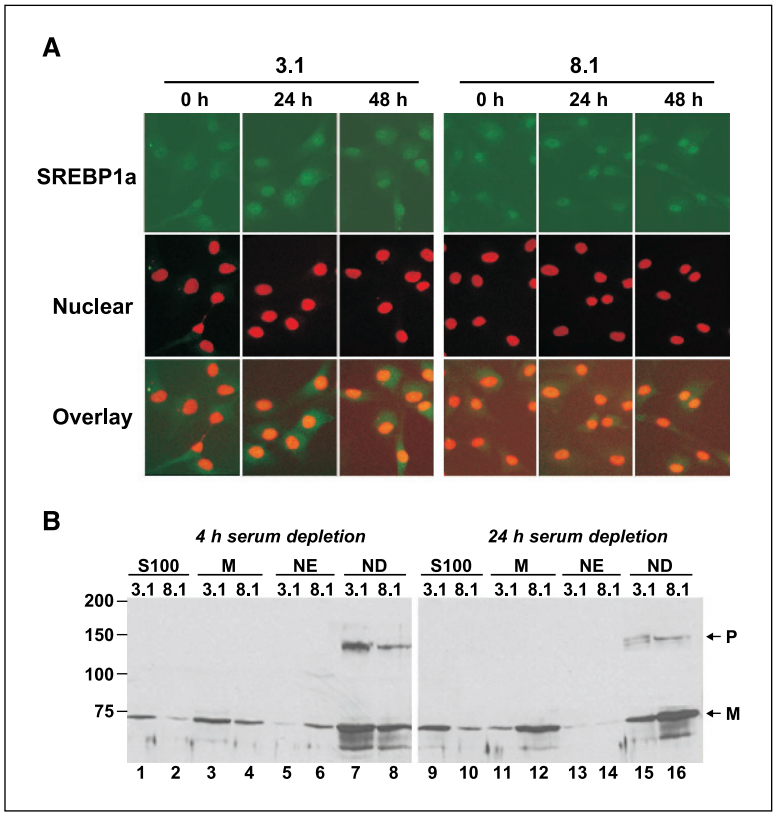

Figure 4. PDGF autocrine signaling is not required for proteolytic activation or nuclear translocation of SRE-BP-1a. *A,* clone 3.1 and 8.1 cells were plated, subjected to the indicated duration of serum deprivation, and then stained for the presence of SRE-BP-1a (*top*) as described in Materials and Methods. Nuclei were stained with H-33342 and pseudocolored in *red* (*center*). Merged images of SRE-BP-1a and H-33342 are shown at the *bottom* (overlay). *B,* immunoblot analysis of subcellular distribution of SRE-BP-1a in U87 clones following serum deprivation. Subcellular fractionation was conducted on cells exposed to either 4 hours (*left*) or 24 hours (*right*) of serum deprivation. Equivalent quantities (20 μg protein) from cytosol (*S100*), membrane (*M*), nuclear extract (*NE*), and nuclear debris (*ND*) fractions of clone 3.1 and 8.1 cells were analyzed for SRE-BP-1a content by immunoblotting. *P,* SRE-BP precursor; *M,* mature processed form.

exhibited the degree of PDGF dependence of cluster 1 obtained above. Thus, all further assessments were conducted with clusters 1 and 2, derived from the autocrine PDGF-regulated gene list.

To compare the genotypic and clinical features of clusters 1 and 2 (Table 2), the analysis was restricted to 50 tumors (22) obtained from patients who had yet to receive treatment ("nonrecurrent" tumors) to avoid the potential complicating factor of therapeutic intervention. Thirty-two of these gliomas corresponded to cluster 1 (12 glioblastomas and 20 anaplastic oligodendrogliomas), with the remaining 18 (16 glioblastomas and 2 anaplastic oligodendrogliomas) belonging to cluster 2. Six different genotypic markers were examined: loss of heterozygosity (LOH) at 1p, 19q, and 10q, homozygous deletion (HD) of the tumor suppressor *p16/CDKN2A* gene, amplification of the epidermal growth factor receptor (*EGFR*) gene, and mutations within the *TP53* gene. None of the 32 gliomas within cluster 1 displayed *EGFR* gene amplification compared with 44% of cluster 2 tumors. Also striking was the small percentage of cluster 1 tumors exhibiting LOH at 10q relative to cluster 2 (11% versus 79%). LOHs at 1p and 19q as well as TP53 mutations were observed more frequently in cluster 1 tumors, whereas HD of the *p16/CDKN2A* gene was seen more frequently in cluster 2. All of these genotypic distinctions between clusters 1 and 2 were retained within the glioblastoma subgroup, with TP53 mutations present at a particularly higher rate in the glioblastomas of cluster 1 (50% versus 19%). A lack of sample size within cluster 2

Table 2. Genotypic features of glioma subgroups clustered by degree of PDGF-dependent gene expression

Genotype	All gliomas		Glioblastomas		Anaplastic oligodendrogliomas	
	Cluster 1	Cluster 2	Cluster 1	Cluster 2	Cluster 1	Cluster 2
1p LOH	13/30 (43)	2/14 (14)	4/10 (40)	1/12 (8)	9/20 (45)	1/2 (50)
19q LOH	11/29 (38)	3/14 (21)	5/12 (42)	3/12 (25)	6/17 (35)	0/2 (0)
10q LOH	3/27 (11)	11/14 (79)	2/9 (22)	9/12 (75)	1/18 (6)	2/2 (100)
p16 HD	5/31 (16)	8/17 (47)	2/11 (18)	6/15 (40)	3/20 (15)	2/2 (100)
EGFR amplification	0/32 (0)	8/18 (44)	0/12 (0)	8/16 (50)	0/20 (0)	0/2 (0)
p53 mutant	10/30 (33)	3/18 (17)	5/10 (50)	3/16 (19)	5/20 (25)	0/2 (0)

NOTE: Shown are the ratios of tumors exhibiting the indicated genotypes divided by the total number of tumors analyzed. The corresponding percentages are given in parentheses.

of anaplastic oligodendrogliomas precluded reliable genotypic comparisons for the anaplastic oligodendroglioma tumor subgroup. Analysis of patient data revealed a modest increase in survival time for patients from cluster 1 ($P \leq 0.038$; Fig. 5*A*). Because the majority of anaplastic oligodendrogliomas, tumors known to result in a much worse prognosis than glioblastomas, were found in cluster 1, survival times for patients with glioblastomas and anaplastic oligodendrogliomas were examined independently. Survival times within these two subgroups were not significantly different between the clusters, likely due to insufficient sample number, as cluster 1 tumors of both subtypes exhibited a trend toward increased survival at the tails of their respective survival curves (Fig. 5*B* and *C*). This strongly suggests that the increase in survival of patients within cluster 1 was due at least in part to the PDGF dependence of these tumors and not wholly attributable to the prevalence of anaplastic oligodendrogliomas in the cluster.

Discussion

Little is currently known regarding the patterns of gene expression controlled by autocrine growth factor signaling in cancer. Most studies to date have involved the administration of exogenous agents or forced expression of growth factors and/or receptors, approaches that may not accurately reflect regulation exerted by chronically activated autocrine growth loops. The dominant-negative mutant form of PDGF-A (A^{dn}) has provided a unique tool for identifying genes regulated specifically by PDGF autocrine signaling. By dimerizing with endogenous PDGF monomers before they can form biologically active dimers, both internal and external modes of PDGFR activation are inhibited, enabling a comparison of gene expression profiles in the presence and absence of the PDGF autocrine loop. Moreover, because dimerization of PDGF subunits is highly specific, the A^{dn} polypeptide provides a more selective blockade of PDGF signaling than might be expected from synthetic inhibitors or antagonists. It should be noted that the PDGF-C and PDGF-D isoforms, which only homodimerize and would thus not be targeted by the A^{dn} polypeptide, have also been implicated in autocrine growth stimulation in glioblastoma (11). Thus, the profound effects of A^{dn} expression on gene expression and malignant growth in U87 cells indicate unique contributions of PDGF-A and PDGF-B to the autocrine signaling process but do not exclude additional participation by PDGF-C and PDGF-D. Most of the genes regulated by PDGF autocrine activity in U87 cells seem to be novel, not identified previously as transcriptional targets of PDGF. In the only comprehensive analysis of PDGF-dependent gene expression reported to date, Fambrough et al. (26) identified 66 immediate early genes that were induced following in response to ligand-activated PDGFRβ in mouse NIH-3T3 fibroblasts. A listing of genes identified in the current study that were documented previously to be regulated by PDGF action is shown in Supplementary Table S2. For most of these, the expected form of regulation was observed in our experiments. Genes involved with cholesterol synthesis and uptake were consistently up-regulated, consistent with earlier reports of PDGF induction of two such genes, *LDL receptor* and *HMG-CoA reductase*. Also consistent with previous studies was the autocrine PDGF-mediated up-regulation of versican 3 and ornithine decarboxylase as well as the down-regulation of *angiopoietin-1* and *MT-MMP*. However, autocrine PDGF signaling repressed the expression of four genes shown previously to be up-regulated by PDGF (*TSP-1, type IV collagen, ICAM*, and *Notch 3*). In regard to genes regulated only by treatment with exogenous PDGF, much better agreement was observed with previous literature reports (10 of 12). Also noteworthy was the consistency in directionality of regulation (i.e., up-regulation versus down-regulation) for all 27 genes that were regulated by both autocrine and exogenous PDGF. A remarkable degree of agreement was also apparent in the degree of expressional control (fold change) observed for many of these genes [e.g., compare *TSSC3, MPD, HMG-CoA synthase*, and *fatty acid desaturase 2* (*FADS2*); Table 1].

Although this study revealed a high number and broad spectrum of PDGF-regulated genes, the induction of genes involved in biosynthesis and uptake of cholesterol and isoprenoids was particularly striking. We showed that this coordinate induction was likely to be mediated at least in part by the SREs of these target genes (34). Our studies yielded the surprising result, however, that proteolytic activation and nuclear translocation of the cognate transcription factor, SRE-BP-1a, continued even in the absence of PDGF autocrine signaling. This suggests that PDGFR provides an additional signal required for transcriptional activation of these genes. In this regard, SRE-BPs are substrates for ERK1 and ERK2 phosphorylation *in vitro* (47). PDGF autocrine activity induced not only cholesterol/lipid biosynthetic and transport genes but also two genes with accessory functions in the SRE-BP activation pathway itself. One of these was *insulin-induced protein 1* (*INSIG-1*), a protein involved in retention of latent SRE-BP within the ER. *INSIG-1* is itself a SRE-BP-inducible gene (48), suggesting a negative feedback function in the cellular response to low sterol levels. Another was interleukin-1β converting enzyme (ICE)–related protease, shown previously to cleave SRE-BP-1 and SRE-BP-2 *in vitro* at the same site targeted *in vivo* (35). Interestingly, this

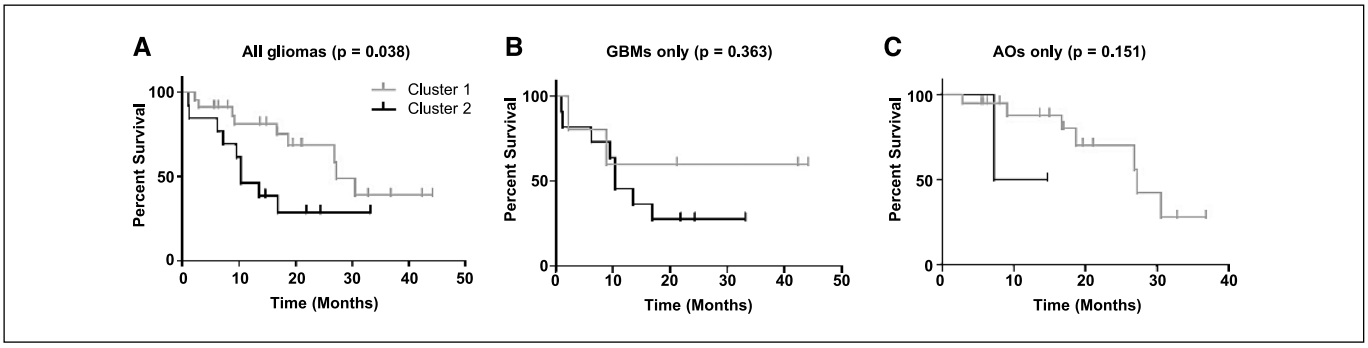

Figure 5. Survival curves of glioma cluster 1 (*gray*) and cluster 2 (*black*). *A,* all gliomas; *B,* glioblastomas (*GBMs*) only; *C,* anaplastic oligodendrogliomas (*AOs*) only.

protease corresponds to neither site-1 protease or site-2 protease, the Golgi-localized enzymes more recently identified as the main activators of SRE-BP (49).

The profile of gene expression regulated by PDGF autocrine activity in the glioblastoma-derived cell line U87 has been proven to be a useful predictor of gene expression patterns in a subgroup (cluster 1) of human glial tumors. A particularly high degree of correlation was found with respect to the regulation of genes required for cholesterol and lipid homeostasis. PDGF-dependent tumors may thus have an elevated demand for the products of the mevalonate pathway, such as cholesterol for membrane synthesis as well as isoprenoids for prenylation of Ras and other related small G proteins. Our observations raise the interesting possibility that cluster 1 gliomas may be especially sensitive to inhibitors of HMG-CoA reductase and farnesyltransferases, particularly blood-brain barrier–permeable agents, such as simvastatin (50). Statins exhibit antiproliferative and proapoptotic activities against several different tumor cell lines in culture (51), including U87 and A172 astrocytoma cells (52). Cluster 1 gliomas also displayed several intriguing genotypic patterns, the most striking of which was an absence of EGFR amplification. This strongly suggests that constitutive receptor tyrosine kinase (RTK) signaling plays a critical role in gliomagenesis, with either PDGF autocrine activity or *EGFR* gene amplification representing independent modes of satisfying this requirement. It is tempting to speculate that gliomas, which exhibit neither PDGF autocrine signaling nor *EGFR* gene amplification, will have acquired constitutive RTK activity via related receptors or mechanisms. The lesion underlying establishment of constitutive autocrine PDGF activity in glial tumors is poorly understood. *PDGFR* gene amplification has been documented but is much rarer than that of EGFR (10). However, that study also highlighted an intriguing relationship between the coincident appearance of PDGF autocrine activity and TP53 mutations (and LOH on chromosome 17p) in low-grade gliomas, suggesting a functional connection between these events. Moreover, mice that are homozygous null for either p53 or p16 (Ink4a-Arf) yield glioblastoma-like tumors in response to retrovirally delivered PDGF-B at a higher frequency and exhibit shorter latency than wild-type mice (53). This indicates important functional cooperativity between PDGF autocrine loop activity and inactivation of these important tumor suppressor genes. Our observation that the PDGF-dependent gliomas of cluster 1 harbored a significantly higher proportion of TP53 mutations, particularly within the glioblastoma subgroup, provides functional evidence in support of such a relationship. In contrast, cluster 1 tumors exhibited a lower rate of HD of the *p16* gene, suggesting that although functional collaboration with PDGF autocrine activity is possible it does not seem to represent a favored route to glial malignancy. Other genotypic features of cluster 1 tumors (increased LOH at 1p and 19q and decreased LOH at 10q) are also of interest and worthy of future study.

In summary, these studies show that PDGF autocrine loop activity represents a master regulator of gene transcription patterns in cultured glioblastoma cells. Many of the genes identified have been implicated previously in the promotion or suppression of malignant growth and thus represent novel and rational targets for the glioma therapy. Moreover, the database of comprehensive gene expression profiles reported herein, in conjunction with detailed genotypic and prognostic correlates in tumors from human glioma patients, should provide a valuable resource for studies and treatment of this currently intractable form of human cancer.

Acknowledgments

Received 7/26/2004; revised 4/8/2005; accepted 4/12/2005.

Grant support: NIH grants CA 83237, HL 62877, and AG 10836 (D. Kaetzel) and CA 57683 (D. Louis) and Kentucky Lung Cancer Research Board (D. Kaetzel).

The costs of publication of this article were defrayed in part by the payment of page charges. This article must therefore be hereby marked *advertisement* in accordance with 18 U.S.C. Section 1734 solely to indicate this fact.

We thank Dr. Arnold Stromberg for statistical assistance, Dr. Timothy Osborne (University of California, Irvine) for kindly providing the SRE and SRE-BP expression and reporter plasmids, Dr. Nathalie Lokker for the gift of CT52923, Drs. Doug Andres and Skip Waechter for helpful discussions and advice, and Dr. Eric Blalock for expert assistance with computer graphics.

References

1. Maher EA, Furnari FB, Bachoo RM, et al. Malignant glioma: genetics and biology of a grave matter. Genes Dev 2001;15:1311–33.
2. Heldin C-H, Westermark B. Mechanism of action and *in vivo* role of platelet-derived growth factor. Physiol Rev 1999;79:1283–316.
3. LaRochelle WJ, Jeffers M, McDonald WF, et al. PDGF-D, a new protease-activated growth factor. Nat Cell Biol 2001;3:517–21.
4. Gilbertson DG, Duff ME, West JW, et al. Platelet-derived growth factor C (PDGF-C), a novel growth factor that binds to PDGF α and β receptor. J Biol Chem 2001; 276:27406–14.
5. Heldin C-H, Westermark B. Platelet-derived growth factor: mechanism of action and possible *in vivo* function. Cell Regul 1990;1:555–66.
6. Hermanson M, Funa K, Hartman M, et al. Platelet-derived growth factor and its receptors in human glioma tissue: expression of messenger RNA and protein suggests the presence of autocrine and paracrine loops. Cancer Res 1992;52:3213–9.
7. Claesson-Welsh L. Platelet-derived growth factor receptor signals. J Biol Chem 1994;269:32023–6.
8. Fleming TP, Matsui T, Heidaran MA, et al. Demonstration of an activated platelet-derived growth factor autocrine pathway and its role in human tumor cell proliferation *in vitro*. Oncogene 1992;7:1355–9.
9. Maxwell M, Naber SP, Wolfe HJ, et al. Coexpression of platelet-derived growth factor (PDGF) and PDGF-receptor genes by primary human astrocytomas may contribute to their development and maintenance. J Clin Invest 1990;86:131–40.
10. Hermanson M, Funa K, Koopmann J, et al. Association of loss of heterozygosity on chromosome 17p with high platelet-derived growth factor α receptor expression in human malignant gliomas. Cancer Res 1996;56: 164–71.
11. Lokker NA, Sullivan CM, Hollenbach SJ, Israel MA, Giese NA. Platelet-derived growth factor (PDGF) autocrine signaling regulates survival and mitogenic pathways in glioblastoma cells: evidence that the novel PDGF-C and PDGF-D ligands may play a role in the development of brain tumors. Cancer Res 2002;62: 3728–35.
12. Vassbotn FS, Andersson M, Westermark B, Heldin C-H, Ostman A. Reversion of autocrine transformation by a dominant negative platelet-derived growth factor mutant. Mol Cell Biol 1993;13:4066–76.
13. Shamah SM, Stiles CD, Guha A. Dominant-negative mutants of platelet-derived growth factor revert the transformed phenotype of human astrocytoma cells. Mol Cell Biol 1993;13:7203–12.
14. Schilling D, Reid JDI, Hujer A, et al. Loop III region of platelet-derived growth factor (PDGF) B-chain mediates binding to PDGF receptors and heparin. Biochem J 1998; 333:637–44.
15. Kaetzel DM, Reid JD, Pedigo N, Zimmer SG, Boghaert ER. A dominant-negative mutant of the platelet-derived growth factor A-chain increases survival of hamsters implanted with the highly invasive CxT24-neo3 glioblastoma cell. J Neurooncol 1998;39:33–46.
16. Kilic T, Alberta JA, Zdunek PR, et al. Intracranial inhibition of platelet-derived growth factor-mediated glioblastoma cell growth by an orally active kinase inhibitor of the 2-phenylaminopyrimidine class. Cancer Res 2000;60:5143–50.
17. Keating MT, Williams LT. Autocrine stimulation of intracellular PDGF receptors in v-*sis* transformed cells. Science 1988;239:914–6.
18. Bejcek BE, Li DY, Deuel TF. Transformation by v-*sis* occurs by an internal autoactivation mechanism. Science 1989;245:1496–9.
19. Fleming TP, Matsui T, Molloy CJ, Robbins KC, Aaronson SA. Autocrine mechanism for v-*sis* transformation requires cell surface localization of internally activated growth factor receptors. Proc Natl Acad Sci U S A 1989;86:8063–7.
20. Hannink M, Donoghue DJ. Autocrine stimulation by the v-*sis* gene product requires a ligand-receptor interaction at the cell surface. J Cell Biol 1988;107: 287–98.
21. Blalock EM, Chen KC, Sharrow K, et al. Gene microarrays in hippocampal aging: statistical profiling identifies novel processes correlated with cognitive impairment. J Neurosci 2003;23:3807–19.

22. Nutt CL, Mani DR, Betensky RA, et al. Gene expression-based classification of malignant gliomas correlates better with survival than histological classification. Cancer Res 2003;63:1602–7.
23. Fenstermaker RA, Poptic E, Bonfield TL, et al. A cationic region of the platelet-derived growth factor (PDGF) A-chain (Arg^{159}-Lys^{160}-Lys^{161}) is required for receptor binding and mitogenic activity of the PDGF-AA homodimer. J Biol Chem 1993;268:10482–9.
24. Fambrough D, McClure K, Kazlauskas A, Lander ES. Diverse signaling pathways activated by growth factor receptors induce broadly overlapping, rather than independent, sets of genes. Cell 1999;97:727–41.
25. Royer-Pokora B, Loos U, Ludwig WD. TTG-2, a new gene encoding a cysteine-rich protein with the LIM motif, is overexpressed in acute T-cell leukaemia with the t(11;14)(p13;q11). Oncogene 1991;6:1887–93.
26. Ishii H, Vecchione A, Murakumo Y, et al. FEZ1/LZTS1 gene at 8p22 suppresses cancer cell growth and regulates mitosis. Proc Natl Acad Sci U S A 2001;98:10374–9.
27. Lawler J. Thrombospondin-1 as an endogenous inhibitor of angiogenesis and tumor growth. J Cell Mol Med 2002;6:1–12.
28. Amagasaki K, Sasaki A, Kato G. Antisense-mediated reduction in thrombospondin-1 expression reduces cell motility in malignant glioma cells. Int J Cancer 2001; 94:508–12.
29. Tenan M, Fulci G, Albertoni M, et al. Thrombospondin-1 is downregulated by anoxia and suppresses tumorigenicity of human glioblastoma cells. J Exp Med 2000;191:1789–98.
30. Marneros AG, Olsen BR. The role of collagen-derived proteolytic fragments in angiogenesis. Matrix Biol 2001; 20:337–45.
31. Manda R, Kohno T, Niki T, et al. Differential expression of the LAMB3 and LAMC2 genes between small cell and non-small cell lung carcinomas. Biochem Biophys Res Commun 2000;275:440–5.
32. Cao Y. Endogenous angiogenesis inhibitors and their therapeutic implications. Int J Biochem Cell Biol 2001; 33:357–69.
33. Horton JD, Goldstein JL, Brown MS. SREBPs: activators of the complete program of cholesterol and fatty acid synthesis in the liver. J Clin Invest 2002;109: 1125–31.
34. Wang X, Pai JT, Wiedenfeld EA, et al. Purification of an interleukin-1β converting enzyme-related cysteine protease that cleaves sterol regulatory element-binding proteins between the leucine zipper and transmembrane domains. J Biol Chem 1995;270:18044–50.
35. Lund EG, Kerr TA, Sakai J, Li WP, Russell DW. cDNA cloning of mouse and human cholesterol 25-hydroxylases, polytopic membrane proteins that synthesize a potent oxysterol regulator of lipid metabolism. J Biol Chem 1998;273:34316–27.
36. Barker PA, Salehi A. The MAGE proteins: emerging roles in cell cycle progression, apoptosis, and neurogenetic disease. J Neurosci Res 2002;67:705–12.
37. Scanlan MJ, Jager D. Challenges to the development of antigen-specific breast cancer vaccines. Breast Cancer Res 1903;3:95–8.
38. Alberti S, Miotti S, Stella M, et al. Biochemical characterization of Trop-2, a cell surface molecule expressed by human carcinomas: formal proof that the monoclonal antibodies T16 and MOv-16 recognize Trop-2. Hybridoma 1992;11:539–45.
39. Senner V, Sturm A, Baur I. CD24 promotes invasion of glioma cells *in vivo*. J Neuropathol Exp Neurol 1999; 58:795–802.
40. Alho H, Kolmer M, Harjuntausta T, Helen P. Increased expression of diazepam binding inhibitor in human brain tumors. Cell Growth Differ 1995;6:309–14.
41. Repa JJ, Liang G, Ou J, et al. Regulation of mouse sterol regulatory element-binding protein-1c gene (SREBP-1c) by oxysterol receptors, LXRα and LXRβ. Genes Dev 2000;14:2819–30.
42. Wu LC, Wang ZW, Tsan JT, et al. Identification of a RING protein that can interact *in vivo* with the BRCA1 gene product. Nat Genet 1996;14:430–40.
43. Zhou H, Kuang J, Zhong L, et al. Tumour amplified kinase STK15/BTAK induces centrosome amplification, aneuploidy and transformation. Nat Genet 1998;20:189–93.
44. Yamashita Y, Kajigaya S, Yoshida K, et al. Sak serine-threonine kinase acts as an effector of Tec tyrosine kinase. J Biol Chem 2001;276:39012–20.
45. Vallett SM, Osborne TF. Two separate sites contribute to AP-1 activation of the promoter for 3-hydroxy-3-methylglutaryl coenzyme A synthase. Nucleic Acids Res 1994;22:5184–9.
46. Yu JC, Lokker NA, Hollenbach S, et al. Efficacy of the novel selective platelet-derived growth factor receptor antagonist CT52923 on cellular proliferation, migration, and suppression of neointima following vascular injury. J Pharmacol Exp Ther 2001;298:1172–8.
47. Kotzka J, Muller-Wieland D, Roth G, et al. Sterol regulatory element binding proteins (SREBP)-1a and SREBP-2 are linked to the MAP-kinase cascade. J Lipid Res 2000;41:99–108.
48. Yabe D, Brown MS, Goldstein JL. Insig-2, a second endoplasmic reticulum protein that binds SCAP and blocks export of sterol regulatory element-binding proteins. Proc Natl Acad Sci U S A 2002;99:12753–8.
49. Goldstein JL, Rawson RB, Brown MS. Mutant mammalian cells as tools to delineate the sterol regulatory element-binding protein pathway for feedback regulation of lipid synthesis. Arch Biochem Biophys 2002;397:139–48.
50. Saheki A, Terasaki T, Tamai I, Tsuji A. *In vivo* and *in vitro* blood-brain barrier transport of 3-hydroxy-3-methylglutaryl coenzyme A (HMG-CoA) reductase inhibitors. Pharm Res 1994;11:305–11.
51. Wong WW, Dimitroulakos J, Minden MD, Penn LZ. HMG-CoA reductase inhibitors and the malignant cell: the statin family of drugs as triggers of tumor-specific apoptosis. Leukemia 2002;16:508–19.
52. Jones KD, Couldwell WT, Hinton DR, et al. Lovastatin induces growth inhibition and apoptosis in human malignant glioma cells. Biochem Biophys Res Commun 1994;205:1681–7.
53. Hesselager G, Uhrbom L, Westermark B, Nister M. Complementary effects of platelet-derived growth factor autocrine stimulation and p53 or Ink4a-Arf deletion in a mouse glioma model. Cancer Res 2003;63:4305–9.